Available online at www.sciencedirect.com

ScienceDirect

Procedia CIRP 119 (2023) 158–163

www.elsevier.com/locate/procedia

33rd CIRP Design Conference

Digital Twins towards Microwave-assisted 3D Printing of Continuous Carbon Fiber Reinforced Composites

Nanya Li[a]*, Guido Link[a], John Jelonnek[a], S. K. Ong[b]

a Institute for Pulsed Power and Microwave Technology, Karlsruhe Institute of Technology, Eggenstein-Leopoldshafen, 76344, Germany
b Department of Mechanical Engineering, National University of Singapore, 9 Engineering Drive 1, Singapore, 117576, Singapore

* Corresponding author. Tel.: +49 721 608-23620. *E-mail address: nanya.li@outlook.com*

Abstract

Microwave-assisted 3D printing based on the fused filament fabrication (FFF) method is an emerging technology to print lightweight continuous carbon fiber reinforced thermoplastics (CCFRP) at high speed. Different from traditional FFF, microwave offers selective and volumetric heating properties to melt thermoplastic materials instantaneously, and the microwave printing head and nozzle remain at room temperature. These advantages can increase the printing speed of CCFRP significantly, while the belt slippage of a printing bed is noticed during microwave-assisted 3D printing. The slippage of the moving belt happens because the cold nozzle moves at high speed and encounters resistance from the rough surface of the printed filament. To solve this problem, this paper presents a hierarchical digital twin (DT) framework, consisting of core and basic DTs, for the prevention of belt slippage induced printing malfunction. The core DTs use MATLAB Simscape multibody models to simulate the printing process virtually and the printing G-code is corrected before printing. In addition, an accelerometer installed on the printing bed is connected to the core DTs. Abnormal vibration signals due to belt slippage can be measured and communicated with core DTs for interrupting and correcting the process. By monitoring the temperature of the heated filament and the output microwave power, the service life of the nozzle and microwave cable are evaluated in the basic DTs.

Keywords: Additive manufacturing; Digital twin; Microwave heating; Process control

1. Introduction

3D printing technologies are used increasingly to produce end-use plastics, metals and fiber reinforced composites [1-3]. Lightweight continuous carbon fiber reinforced plastic (CCFRP), which has higher stiffness and fatigue strength compared to structures made of metal [4], has been widely used in the lightweight industry, in particular in the field of mobility, for example, electrical vertical take-off and landing (eVTOL) aircraft manufacturing and internal combustion engine (ICE) vehicles fabrication, etc. [5]. Compared to the conventional 3D printing methods, such as fused filament fabrication (FFF) [6], the 3D microwave printing method presented by the author is assisted by microwave heating and shows huge potential to increase the printing speed, printing dimension, and mechanical properties of CCFRP [7]. Different from metallic components produced by laser sintering [8], the 3D microwave printing of CCFRP can manipulate the fiber orientation and material distribution to allow for maximum weight reduction [9]. The authors presented the 3D microwave printing method and developed the first prototype called "SERPENS" to manufacture CCFRP components in high speed [10]. As the printing head of the SERPENS printer is connected to a solid-state microwave power source by using an inflexible coaxial cable, the printing head only moves in the Z-direction to avoid bending the cable. Therefore, the printing bed has to move in X- and Y-directions. This unique motion mechanism requires two sets of stepper motors and pulley-belts that are installed

10.1016/j.procir.2023.03.088

under the printing bed and increases the weight of the printing bed. However, the pulley-belt system is more suitable for low payload conditions. While the cold printing head moves at high speed, the nozzle encounters resistance from the rough surface of the printed filament and leads to belt slippage problems. Furthermore, the belt slippage induces fiber misalignment and printing failure.

Digital twin (DT) technology has been in use since 1960 to create a duplicate of a physical system and test its functions in a virtual environment [11,12]. For both the design stage and the manufacturing process, DT technology creates new opportunities to solve the challenges mentioned above. As reported, multibody simulation and modeling of a system is the best way to mirror the life of its corresponding physical twin [13]. Additive manufacturing of metallic parts uses DT technology to reduce trial-error testing and make printing cost-effective [14]. The capability to capture a large amount of data allows for in-line inspection and analysis, which provides a new avenue to determine the correlation of the process parameters with the production quality [15]. Correlating the simulation results to a real physical structure [16], the relationships between the factors can be identified. For risk evaluation, a virtual verification using a digital production twin allows early estimations even before the actual ramp-up of the production [17].

The paradigm of DT modeling of additive manufacturing of metals has been researched and reported. However, the main challenges of 3D microwave printing of CCFRP have not been researched yet and DT technology could be a promising approach to solve them. Motivated by this need, this paper proposes a novel hierarchical DT framework of the authors' 3D microwave printing system. This hierarchical DT framework, which consists of core DTs and basic DTs, is capable of specifying the motion of the belt on each axis according to a defined printing path and predicting the malfunction risk due to belt slippage. An accelerometer is attached to the printing bed to detect its acceleration signals for distinguishing the belt slippage of the printing bed. The 3-axis acceleration signals are acquired, transformed, and filtered in digital form using "Wire" and "Kalman filter" libraries in Arduino and are manipulated by the core DTs, which are built in the environment of MATLAB. Bi-directional data transfer and real-time communication between the physical and virtual objects have been achieved. Once the belt slippage is detected by the core DTs, an emergency stop command is sent to the SERPENS control system for suspending the printing process. In addition, by measuring the nozzle temperature and microwave transmission power, the service life of the nozzle and microwave cable are evaluated in the basic DTs.

2. 3D microwave printing of lightweight CCFRP

A 3D microwave printing system named "SERPENS" mainly includes a specialized single-mode resonant microwave cavity, which are integrated into a three-axis CNC (computer numerical control) machine [10]. The carbon fibers inside the filament are strong absorbers of microwaves due to the Joule heating of induced current on their skin. In order to adjust the microwave power quickly, a 300 W, 2.4 to 2.5 GHz solid-state microwave generator controlled by pulsed modulation has been used. An Anritsu inline peak power sensor and an MPU6050 accelerometer have been integrated to measure the microwave power and the acceleration of the printing bed. The MPU6050 accelerometer is a motion tracking sensor and combines a 3-axis gyroscope and a 3-axis accelerometer in a very compact package. Here, the 3-axis acceleration module is working under the principle of piezoelectric effect. The module captures the acceleration value by measuring the inertial force applied to a mass block during acceleration. At the software level, a web browser-based interface displays all the data and information in real-time, communicates with a local server, and aims to control, analyse, and monitor the printing process. A safety cut-off function of the microwave power is applied by monitoring the filament heating temperature with a pre-defined threshold. If the temperature exceeds this threshold, the power will be shut down to prevent the burning of the filament inside the cavity. The printing path of composite structures has been planned before the printing process and is simulated in the core DTs before printing to avoid errors. By using the G-code language that controls the CNC machine, the communication between commands and the printing process becomes easier. A modified G-code communication protocol has been written in the local server to unify the control of the path coordinates, speed, microwave power, temperature, cooling, actuator and data logger.

3. Hierarchical DTs framework for 3D microwave printing

Building high fidelity DTs of the 3D microwave printing process to predict the belt slippage requires accurate multibody simulation models. However, these models are computationally intensive and require long computing times. The rapid control loop of 3D printing conflicts with the long computing times of DT models. In this research, a novel hierarchical structure of DTs as shown in Figure 1 has been formulated to solve this problem. It also illustrates the flowchart of this research work.

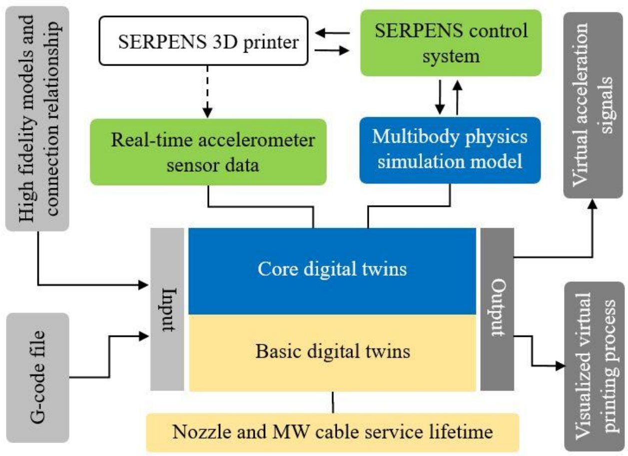

Figure 1. Hierarchical structure of digital twins for 3D microwave printing.

A physical system can involve many DTs for different purposes. The input data are different based on the purpose that these DTs are targeted for. As shown in Figure 1, the input data for the hierarchical DTs are the G-code file and model connection relationships, such as the assembly relation and pulley-belt joints. The core DTs of multibody physics simulation models and an accelerometer sensor are established using MATLAB Simscape, which can run separately from the basic DTs. The motion of the printing bed in X and Y directions is designated as pulley-belt joints, and the Z axis is the lead screw connection between printer frame and printing head. An Arduino Megatronic V3.2 and an Arduino Uno board are applied to connect the SERPENS 3D microwave printing control system, stepper motors and a

MPU6050 accelerometer. The basic DTs can be a service lifetime simulator of printing nozzle and microwave cable based on the input data of nozzle heating temperature and microwave transmission power. The printing nozzle consists of a Teflon sleeve and stainless steel shell, and the variation of filament temperature influences the lifetime of the Teflon sleeve. In addition, cable loss decides how much microwave power can be transmitted to the printing head. Therefore, the service lifetime of microwave cable needs to be monitored as well.

4. Establishment of the core and basic DTs

The core DTs of the 3D microwave printer is established in MATLAB Simscape and shown in Figure 2. The printer has 3 modules and two connection joints, which are the pulley-belt joint and the revolute joint. The world frame is the ground of all frame networks in a mechanical model and the mechanism configuration sets the mechanical and simulation parameters, such as material properties and gravity. The solver configuration defines a "time based equation formulation" and an "absolute/relative tolerance model" for calculating the multibody behaviours.

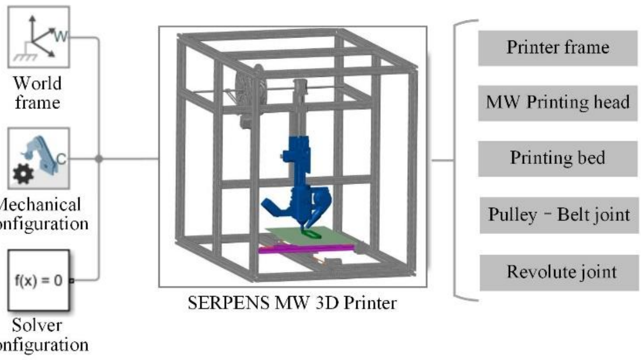

Figure 2. Core DTs of the 3D microwave printer.

As shown in Figure 3, the core DT of the microwave printing head has replicas of the printer frame, microwave (MW) printing head and printing bed. Different from the FFF based conventional 3D printer that has a printing bed that only moves in Z direction, the printing bed of the SERPENS printer has an in-plane freedom. Because the MW printing head connects to the solid-state microwave generator via a coaxial cable and the cable cannot be bent frequently. Thus, the MW printing head is installed on a lead screw guide (prismatic joint) and linearly drives in the Z direction by using a stepper motor, as shown in Figure 3. The pulley-belt joints are applied to connect the printer frame and the printing bed. It is worth noticing that a "Tensioner" is needed to solve the convergence problem of the belt with flexible properties. A motion input is named "Y_motion" and transforms to the revolute angle of the "pulley_Y2" model.

The physical object of the 3D microwave printing system is shown in Figure 4 (a). To obtain a high fidelity DTs of the printing system, all of the aluminium profiles and components, e.g. microwave cavity, infrared camera, cooling ventilator, stepper motors and pulley-belt transmissions are the same as the real objects. As shown in Figure 4 (d) and (e), the printing bed has been installed on two vertical linear guides that are stacked up together. In principle, a heating mat is adhered on the bottom of the printing bed for bed heating. Hence, the bed is hung on four bolts on the corners. Due to the vertically stacked linear guides and the hanging structures, vibration may be induced more easily during the printing process. Meanwhile, the belt of the Y axis is much longer than the X axis, so the chance of belt slippage risk is higher on the Y axis than the X axis, as shown in the Simscape model of Figure 4 (c). A MPU6050 accelerometer is placed on the corner of the printing bed (Figure 4 (b)), it does not affect the printing process and can collect maximum acceleration signals at the same time. The data of the accelerometer and report logs are recorded in a database and sent to the core DTs in MATLAB codes to determine whether the printing process needs to be intervened.

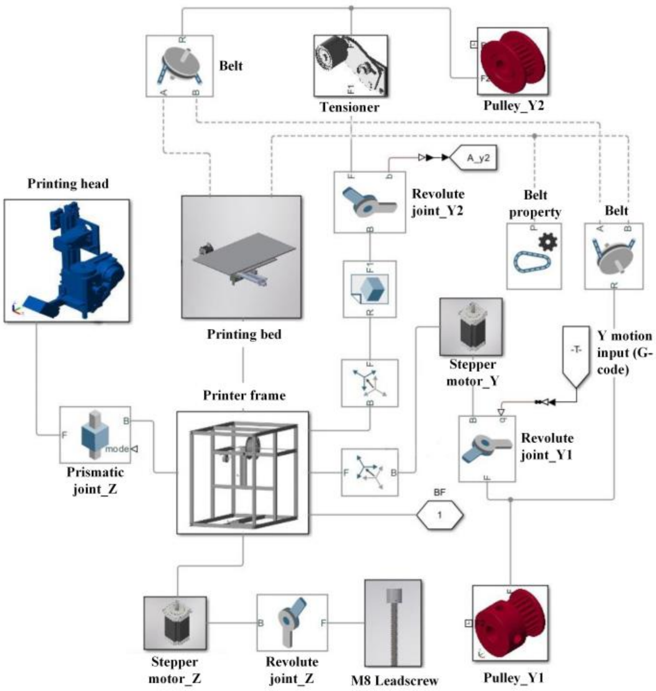

Figure 3. Relationship of the printer frame, MW printing head and printing bed in Simscape.

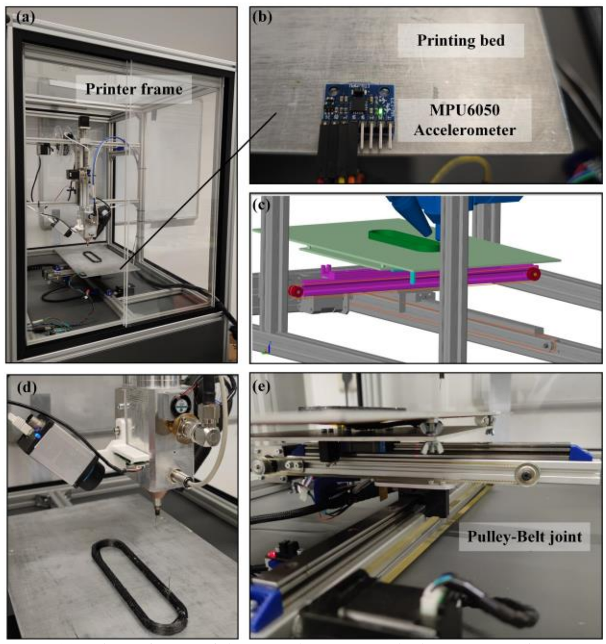

Figure 4. (a) Printer frame of the 3D microwave printing system, (b) MPU6050 accelerometer placed on the printing bed, (c)Simscape simulated pulley-belt joint of the printing bed, (d) MW printing head and the printed O ring composite part, (e) printing bed installed on the pulley-belt joints.

Before the printing process, a G-code printing path of the O ring composite part is simulated in the core DTs for virtual verification. The calculated acceleration values in the Cartesian coordinate system will be analysed. Afterward, the modified G-code file is uploaded to the SERPENS control system, and the data collected from physical sensors are transferred to the DTs in real-time. The historical data is stored in the database to generate general logs, belt slippage risks, service lifetime of nozzle and cable. The modified G-code communication protocol is applied and it also allows to response the inquiry of pulse power modulation rate (on and off time), microwave forward and backward power and the working temperature of the generator. The power loss of the microwave cable is calculated in the basic DTs to evaluate the service lifetime. In addition, the image acquisition toolbox of MATLAB is utilized to communicate with a FLIR infrared camera and outputs the temperature data of hot filaments and the printing nozzle. The thermal heat transferred from hot moving filaments to the Teflon sleeve of the printing nozzle will lead to a softening and degradation of the Teflon material and decrease the service lifetime of the printing nozzle. Thus, the basic DTs will be responsible for monitoring the service lifetime of the nozzle and microwave cable.

5. Results and discussions

The G-code printing path of the O ring composite part is shown in Figure 5 (a), which has a dimension of 161 mm length, 36 mm width and 7 mm thickness (35 layers). By simulating the G-code file in the core DTs, the virtual acceleration values, X_Acc and Y_Acc of the printing bed, are extracted by contains the limits and boundaries of the printing paths, as shown in Figure 5 (c) and (d). It is obvious that the two axes of the accelerometer have different vibration patterns. The positive and negative values refer to relative acceleration and deceleration variations to a static status. The X_Acc axis has acceleration and deceleration peaks very close to each other. However, the Y_Acc axis is more similar to a sine wave, the acceleration and deceleration peaks occur alternately. These patterns follow the geometry feature of the O ring. As shown in Figure 5 (c) and (d), there are lots of high acceleration points that exists on both signals. By analyzing the G-code printing path, the short connection paths in different layers have been found. The short paths jump from one point to another without an appropriate definition of the printing speed and doesn't have the continuity of G^1.

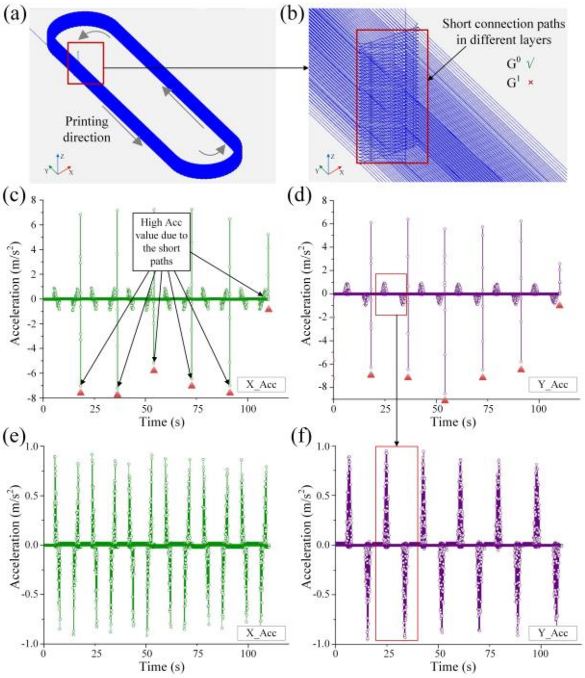

Figure 5. (a) Visualized G-code printing path of the O ring part, (b) short connection paths in different layers that find by core DTs, (c) and (d) calculated X_Acc and Y_Acc acceleration value of the printing bed with the generated G-code, (e) and (f) calculated X_Acc and Y_Acc acceleration value of the printing bed with modified G-code.

By solving this error discovered by virtual verification via DTs, the calculated acceleration signals of X_Acc and Y_Acc are shown in Figure 5 (e) and (f). The abnormal motion behaviour is eliminated from the generated G-code and the vibration patterns can be distinguished easily. Since the printing speed of the straight beams and the circular arcs of the O ring part are the same, the acceleration values of the two axes are nearly the same. In addition, the rigid connections between the components are taken in the Simscape for the core DTs. Hence, the signals induced by elastic deformation of the connection joints cannot be calculated by the core DTs, and that is also the difference between simulated and measured data.

Generally, the 3D microwave printing process starts with a coordinates calibration step. The X, Y, and Z axes of the printer will move to the maximum range and trigger the calibration sensors. This action needs the stepper motors to drive the belts and move the printing bed. The acceleration signals can be recognized by using the MPU6050 accelerometer, as shown in Figure 6. First, the X and Y axes are calibrated and then the Z axis goes down to reach the 0.15 mm gap between the nozzle and printing bed. Afterward, the printing control board reads the G1 linear movement coordinates, and the printing bed moves by following the coordinate commands. As shown in Figure 6 (a), there are 16 acceleration peaks measured in 260 seconds, which indicates the printing has been carried out for 16 circular arc paths.

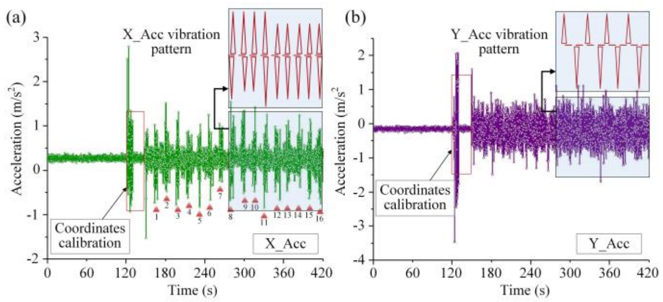

Figure 6. (a) and (b) Measured acceleration signals of the X_Acc and Y_Acc respectively.

The variation ranges of the measured signals changes from -1 m/s^2 to 1.5 m/s^2 and -1.5 m/s^2 to 1 m/s^2 for the X_Acc and Y_Acc of the MPU6050 accelerometer, respectively. By comparing the extracted vibration pattern of the measured signals in Figure 6 (a) and (b) with the calculated results, it can be found that the core DTs predict the correct vibration patterns of the printing bed. Meanwhile, through analyzing the measured acceleration data of multiple experiments, the threshold values are obtained and located on the range of $\pm$ 2.5 m/s^2 for this O ring part.

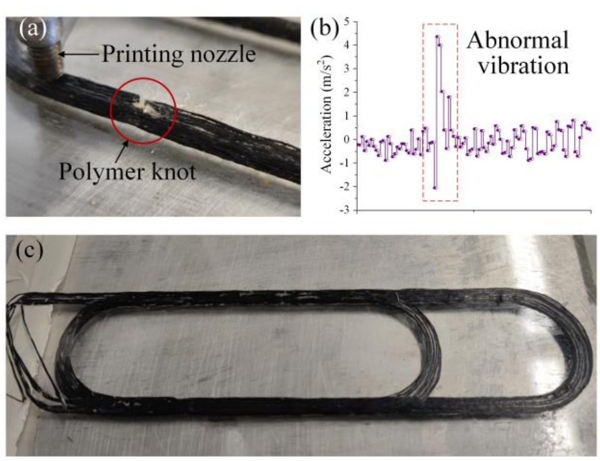

Figure 7. (a) Polymer knot on the printed CCFRP filaments, (b) abnormal vibration due to belt slippage, (c) printing malfunction due to belt slippage.

Lightweight CCFRP manufactured by 3D microwave printing can pave the continuous fibers along the load transmission path and significantly increase the strength/weight ratio. The printed continuous carbon fiber (TORAY 1K 66tex HT T300) reinforced polyamide (Taulman 910 nylon) composite part is demonstrated in Figure 7 (a). During the printing process, a polymer knot is discovered on the top layer of the printed O ring part. This happens exactly in the short connection paths area. The reason is that the sharp turning angle of the filament causes an uneven flow of the polyamide materials in the nozzle even the high acceleration path is eliminated. Because the temperature of the printing nozzle is much lower than the melting temperature of polyamide materials when the nozzle encounters the polymer knot the risk of a belt slippage increases. The vibration signal that is 4 times higher than the normal acceleration value caused by belt slippage is captured and shown in Figure 7 (b). This malfunction during printing leads to the filament misalignment and the O ring CCFRP part cannot be printed appropriately, as demonstrated in Figure 7 (c).

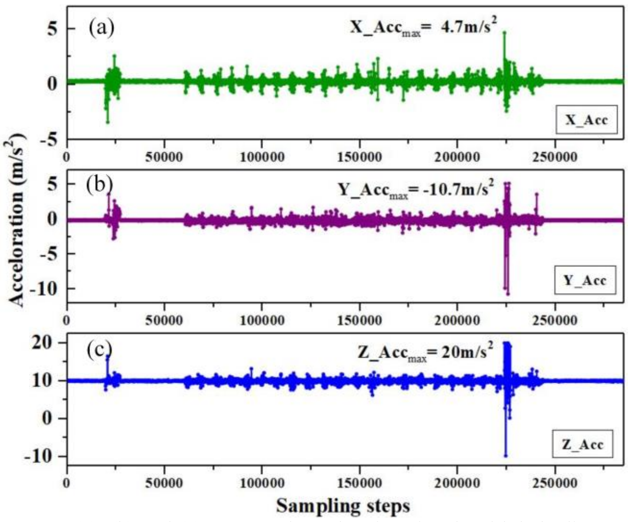

Figure 8. (a), (b) and (c) Measured acceleration signals with belt slippage of the printing bed.

The measured acceleration signals accumulate over time are shown in Figure 8. The accelerometer detects the vibration of the printing bed during 3D microwave printing process accurately. As mentioned before, the first signal is the coordinate calibration and then the printing follows the G-code file to print the CCFRP part layer-by-layer. At the same time, the core and basic DTs start to monitor and control the printing process. The Simscape multibody physical models provide a virtual visualization approach for understanding the influence of printing parameters on the belt slippage risk. It can be seen in Figure 8 that the three axes of the accelerometer have a different response to the dynamic state of the printing bed. The vibration patterns of the X_Acc and Y_Acc are the same as the calculated results of the core DTs, and the Z_Acc is measured by the sensor only. Because the pulley-belt joints connected to the printing bed in the Simscape models cannot output an acceleration signal by considering elastic deformation. Compared with X_Acc and Y_Acc, Z_Acc has a higher acceleration value when the belt slippage happens during printing. Because the vibration transfers from the belt to the bed and leads to significant vertical vibration. When each of the monitored signals goes over the threshold values, which is 2 times higher than the normal acceleration of each axis, the core DTs consider the belt slippage happens and will send the G-code command "M112" for emergency stop and recode the stop points for continuous printing after the error is solved.

To evaluate the service lifetime of the printing nozzle and the microwave cable, the temperature of the filament and the microwave power need to be measured in real-time. As shown in Figure 9 (a), during microwave printing only the continuous carbon fiber reinforced polyamide filament is heated and the thermal heat transfers to the printing nozzle. The filament temperature measured by the infrared camera is illustrated in Figure 9 (b). Due to the view angle of the camera, the filament temperature changes with the printing path. When the filament is hidden by the nozzle, the temperature value decreases, and vice versa. As the moving velocity of the filament in the microwave printing head may have a slight difference with the printing speed, the filament temperature cannot be constant. Once the filament temperature is higher than the maximum usage temperature of the Teflon sleeve, which is about 265°C, the service lifetime of the sleeve in the nozzle will decrease. By involving this evaluation method in the basic DTs, the replacement of the Teflon sleeve can be more efficient and the printing risks are reduced as well.

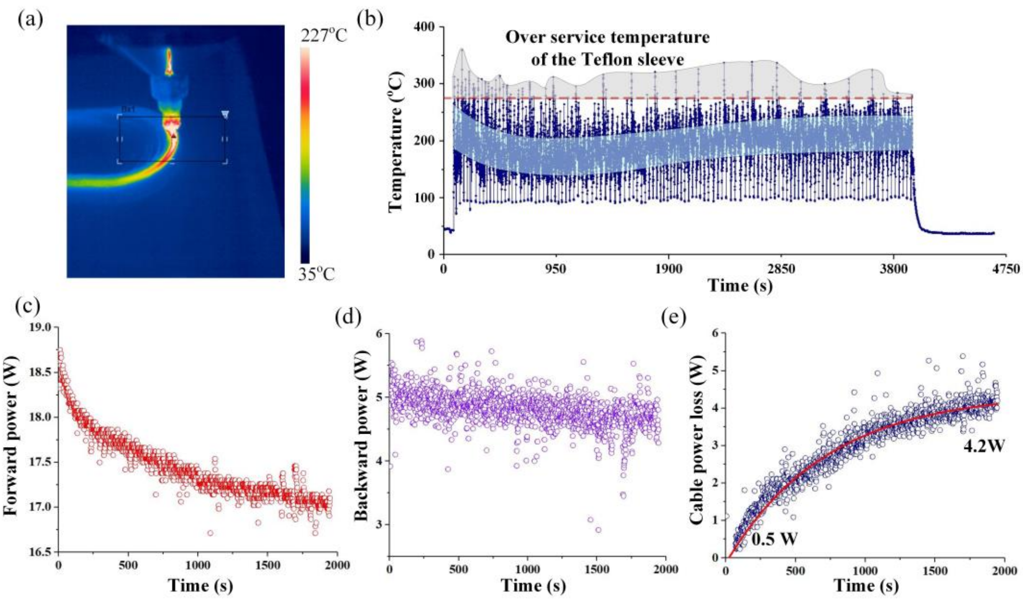

Figure 9. (a) Infrared image of the printing nozzle and microwave heated filament, (b) filament temperature variation during 3D microwave printing, (c), (d) and (e) forward, backward microwave power and evaluated power loss of an aged cable.

In addition, the forward power of the microwave generator will decrease due to an increase in the generator's working temperature. Therefore, the forward power of the generator is decreasing regarding microwave power and working time, as shown in Figure 9 (c). To heat the CCFRP filament that moves under a certain speed to the melting temperature of polyamide material (225ºC), the input power needs to reach 18W. Based on the measured working temperature, a model to calculate the power attenuation of the microwave generator is obtained in basic DTs. Hence, the power is tuned slightly to maintain a nearly stable temperature, as shown in Figure 9 (b).

Furthermore, to transfer the power from the generator to the microwave cavity, the performance of the microwave cable is vital. The maintenance of the MW cable can be achieved by predicting its service lifetime. The basic DTs collect the forward and backward powers and calculate the possible cable power loss, as shown in Figure 9 (d) and (e). The power absorptions on filament materials and the cavity are assumed to be constant. However, the heat dissipation (microwave energy consumption) inside the cavity decreases, because the temperature of the cavity is raising over time. As shown in Figure 9 (e), by testing an aged MW cable, the power loss increases from 0.5 W to 4.2 W after working for 33 minutes. By comparing the power loss of the microwave cable of each printing process, the residual service lifetime of the cable can be predicted to avoid the failure risks of high reflection of microwave due to aged cable.

6. Conclusion and future work

A hierarchical structure composed of core and basic DTs for the 3D microwave printing system has been presented. For the printing malfunction caused by the slippage of motor belts, a key factor of the acceleration data for the printing bed has been found and is monitored in real time. By communicating the monitored data with the core DTs, the belt slippage can be detected immediately. More importantly, the core DTs have a MATLAB Simscape multibody simulation model that can predict the vibration patterns of each axis and correct the G-code path documents before the printing process. By analyzing and comparing the vibration patterns of the measured and calculated data, the core DTs have been verified. Besides, the nozzle and filament temperature are monitored using the infrared imaging method for estimating the service lifetime of the Teflon sleeve inside the nozzle. In addition, the basic DTs calculated the cable power loss based on forward and backward power. The lifetime of the microwave cable can be evaluated as well.

Compared with traditional FFF-based 3D printing processes for continuous carbon fibers, the DTs offer a new way to assure the printing quality of CCFRP and have attractive potential to be further developed for bridging the gap between engineering design and manufacturing. Based on the measured and virtual data of the DTs, the 3D microwave printing process can be well understood and supported by defining specific objectives and constraints for printing paths and process design. Particularly, reducing the iteration periods of engineering designs which focuses on avoiding the risks of printing malfunctions.

This paper is a preliminary research of digital twins towards additive manufacturing of continuous carbon fiber reinforced composite. The DTs have limited communication and reaction to the real microwave-assisted 3D printer. In the future, completely hierarchical DTs based on multibody simulation, accelerometer, and deep learning algorithm will be developed to achieve an intelligent 3D microwave printing of CCFRP part. This new approach is expected to be used in other 3D printing methods for producing high performance and quality components as well.

Acknowledgement

The authors would like to thank the support of the Young Investigator Group Preparation Program (YIG Prep Pro) funding of Karlsruhe Institute of Technology, the establishment of the MATLAB Simscape simulation by Dr. Wenwen Fei from the Dresden University of Technology, and the O ring part STL model provided by Prof. Eric Becker from Arts et Métiers ParisTech.

References

[1] Debroy T, Mukherjee T, Milewski JO, Elmer J, Ribic B, Blecher J, Zhang W. Scientific, technological and economic issues in metal printing and their solutions. Nat Mater 2019;18:1026-1032.

[2] Li N, Link G, Ting W, Ramopoulos V, Neumaier D, Hofele J, Walter M, Jelonnek J. Path-designed 3D printing for topological optimized carbon fiber composite structures. Compos B Eng 2020;182:1-5.

[3] Wang T, Li N, Link G, Jelonnek J, Fleischer J, Dittus J, Kupzik D. Load-dependent path planning method for 3D printing of continuous fiber reinforced plastics. Compos Part A Appl 2020;140:1-11.

[4] Morampudi P, Namala KK, Gajjela YK, Barath M, Prudhvi G. Review on glass fiber reinforced polymer composites. Mater 2021;43:314-319.

[5] Choi J, Jeon J, Lyu J, Park J, Kim G, Chey S, Quan Y, Bhandari B, Prusty G, Ahn S. Current Applications and development of composite manufacturing processes for future mobility. Int J PR Eng Man-GT 2022;1-23.

[6] Ning F, Cong W, Qiu J, Wei J, Wang S. Additive manufacturing of carbon fiber reinforced thermoplastic composites using fused deposition modeling, Compos B Eng 2015;80:369-378.

[7] Li N, Link G, Jelonnek J Rapid 3D microwave printing of continuous carbon fiber reinforced plastics. CIRP Ann Manuf Technol 2020;69:221-224.

[8] Junk S, Klerch B, Hochberg U, Structural optimization in lightweight design for additive manufacturing. Procedia CIRP 2019;84:277-282.

[9] Plakhotnik D, Glasmacher L, Vaneker T, Smetanin Y, Stautner M, Murtezaoglu Y, van Houten F. CAM planning for multi-axis laser additive manufacturing considering collisions. CIRP Ann Manuf Technol 2019;68:447-450.

[10]Li N, Link G, Engler M, Jelonnek J. Small-size coaxial resonant applicator for microwave heating assisted additive manufacturing. IEEE Trans Microw Theory Tech 2021;69:4631-4638.

[11]Cimino C, Negri E, Fumagalli L. Review of digital twin applications in manufacturing. Comput Ind 2019;113:1-15.

[12]Zheng Y, Yang S, Cheng H An application framework of digital twin and its case study. J Ambient Intell Humaniz Comput 2019;10:1141-1153

[13]Tao F, Zhang M, Nee AYC. Digital twin driven smart manufacturing. Academic Press 2019;pp 7-10.

[14]Mukherjee T, DebRoy T. A digital twin for rapid qualification of 3D printed metallic components. Appl Mater Today 2019;14:59-65.

[15]Söderberg R, Wärmefjord K, Carlson J, Lindkvist L. Toward a digital twin for real-time geometry assurance in individualized production. CIRP Ann Manuf Technol 2017;66:137-140.

[16]Huang J, Ong SK, Nee AY. An approach for augmented learning of finite element analysis. Comput Appl in Eng Educ 2019;27/4:921-933.

[17]Wagner R, Schleich B, Haefner B, Kuhnle A, Wartzack S, Lanza G. Challenges and potentials of digital twins and Industry 4.0 in product design and production for high performance products. Procedia CIRP 2019;84:88-93